Combined Therapeutic Effects of Vinblastine and Rapamycin on Human Neuroblastoma Growth, Apoptosis, and Angiogenesis

Danilo Marimpietri,[1] Chiara Brignole,[1] Beatrice Nico,[4] Fabio Pastorino,[1] Annalisa Pezzolo,[1] Federica Piccardi,[3] Michele Cilli,[3] Daniela Di Paolo,[1] Gabriella Pagnan,[1] Luca Longo,[2] Patrizia Perri,[2] Domenico Ribatti,[4] and Mirco Ponzoni[1]

Abstract

Purpose: Vinblastine and rapamycin displayed synergistic inhibition of human neuroblastoma-related angiogenesis. Here, we studied the antitumor activity of vinblastine and rapamycin against human neuroblastoma.

Experimental Design: Cell proliferation, cell cycle progression, and apoptosis were evaluated by measuring ^{3}H-thymidine incorporation, bromodeoxyuridine uptake, and phosphatidylserine exposure, respectively. The *in vivo* sensitivity of neuroblastoma cells to vinblastine and rapamycin was determined in orthotopic neuroblastoma-engrafted mice. Angiogenesis was assessed by the chick embryo chorioallantoic membrane assay.

Results: Each compound alone was able to induce a dose-dependent significant inhibition of cell proliferation, with a dramatically enhanced antiproliferative effect for the drugs used in combination. A marked G_2-M cell cycle arrest with a nearly complete depletion of S phase was associated. The combined treatment triggered an increased apoptosis compared with either drug tested alone. A significant inhibition of tumor growth and microvessel area was obtained in neuroblastoma-bearing mice when treated with vinblastine or rapamycin alone, and a more dramatic effect with the combined treatment, compared with control mice. The therapeutic effectiveness, expressed as increased life span, was statistically improved by the combined therapy, compared with mice treated with either drug tested separately. Histologic evaluation of primary tumors showed that the combined treatment inhibited proliferation and angiogenesis and induced apoptosis. Combined treatment of neuroblastoma cells and neuroblastoma-bearing mice with vinblastine and rapamycin induced the down-modulation of both vascular endothelial growth factor production and vascular endothelial growth factor receptor 2 expression. In the chorioallantoic membrane assay, angiogenesis induced by human neuroblastoma biopsy specimens was significantly inhibited by vinblastine and rapamycin.

Conclusions: These results may be relevant to design new therapeutic strategies against neuroblastoma.

Authors' Affiliations: [1]Laboratory of Oncology, G.Gaslini Children's Hospital; [2]Laboratory of Neuroblastoma Research and [3]Animal Research Facility, Italian Neuroblastoma Foundation c/o National Institute for Cancer Research, Genoa, Italy; and [4]Department of Human Anatomy and Histology, University of Bari, Bari, Italy
Received 11/20/06; revised 4/2/07; accepted 4/18/07.

Grant support: Associazione Italiana per la Ricerca sul Cancro, Fondazione Italiana per la lotta al Neuroblastoma, and Ministry of Health.

The costs of publication of this article were defrayed in part by the payment of page charges. This article must therefore be hereby marked *advertisement* in accordance with 18 U.S.C. Section 1734 solely to indicate this fact.

Note: Supplementary data for this article are available at Clinical Cancer Research Online (http://clincancerres.aacrjournals.org/).

C. Brignole is a recipient of a Fondazione Italiana Ricerca Cancro fellowship. F. Pastorino, G. Pagnan, L. Longo, and P. Perri are recipients of a Fondazione Italiana per la Lotta al Neuroblastoma fellowship.

No sponsor(s) have a role in the design of the study; the collection, analysis, and interpretation of the data; the writing of the manuscript; and the decision to submit the manuscript for publication.

D. Marimpietri and C. Brignole contributed equally to this work and should be considered joint first authors.

Requests for reprints: Mirco Ponzoni, Differentiation Therapy Unit, Laboratory of Oncology, G. Gaslini Children's Hospital, Largo G. Gaslini 5, 16147 Genoa, Italy. Phone: 39-010-5636342; Fax: 39-010-3779820; E-mail: mircoponzoni@ospedale-gaslini.ge.it.

doi:10.1158/1078-0432.CCR-06-2757

Neuroblastoma is the most common extracranial solid tumor of infancy (1). Despite of aggressive treatment strategies, such as high-dose chemotherapy and bone marrow transplantation, the prognosis for patients suffering from advanced stage disease has not been improved in a satisfactory manner and neuroblastoma continues to present a formidable clinical challenge (2). Therefore, development of new treatment approaches has been the focus, in the last few years, of many neuroblastoma studies.

The *Vinca* alkaloid vinblastine is a microtubule inhibitor belonging to an important class of chemotherapeutic agents that affect polymerization and stability of microtubules (3). *Vinca* alkaloids prevent mitotic spindle formation, resulting in a G_2-M phase cell cycle arrest and subsequent apoptotic cell death (4). Vinblastine is mainly used, in combination with other drugs, for therapy of several lymphoid malignancies and some solid pediatric tumors (5, 6).

Rapamycin is a lipophilic macrolide antibiotic, originally identified as an anti-fungal agent. Many studies have, however, showed that rapamycin and its derivatives present both immunosuppressant (7, 8) and antitumor properties (9). Rapamycin acts by specifically inhibiting the mammalian target

of rapamycin protein kinase. The inhibition of mammalian target of rapamycin pathways determines alterations in cell cycle progression, resulting in the blockage of cells in G_1 phase (10–12).

In the last decade, several cytotoxic drugs, already used in the clinical setting, have been investigated for their potential antiangiogenic effects (13). In this respect, it has been recently reported that both vinblastine and rapamycin, tested at low doses, exerted antiangiogenic activity *in vitro* and *in vivo*, through two different mechanisms (14, 15). Furthermore, we have lately shown that vinblastine and rapamycin used in combination, at very low doses, inhibit synergistically human neuroblastoma-related angiogenesis (16). Moreover, proteomic analysis of vinblastine- and rapamycin-treated or untreated endothelial cells allowed us to show that many proteins involved in cell proliferation, migration, apoptosis, and angiogenesis were modulated only by the combined treatment (17).

Vinblastine has been used for chemotherapy of human neuroblastoma, but dose-limiting side effects (i.e., vascular-associated toxicity) have been observed (18). Furthermore, it has been shown that rapamycin inhibited *in vitro* human neuroblastoma cell proliferation (19).

Based on these data, the primary goal of this study was to achieve proof-of-principle for the hypothesis that combined administration of two drugs targeting different phases of the cell cycle results into therapeutic effects superior to those achieved upon treatment with either drug alone. Thus, herein, we have investigated the antitumor activity of both vinblastine and rapamycin tested alone or in combination *in vitro* on a panel of neuroblastoma cell lines and *in vivo* on an orthotopic xenograft mouse model of human neuroblastoma.

Materials and Methods

Chemotherapeutics. Vinblastine (Lilly France SA) was solubilized in PBS and stored at -20°C. Rapamycin (ICN Biomedicals, Inc.) was dissolved in DMSO and kept at -20°C. At the time of use, the drugs were freshly prepared and diluted stepwise, until the desired concentrations, with the culture medium.

Cell lines and culture conditions. The following human neuroblastoma cell lines were used: GI-LI-N (20, 21), HTLA-230 (22), SH-SY5Y (23), ACN (24). All cell lines were used between passages 50 and 75. All cells were grown in complete DMEM, as previously described (25).

Human umbilical vein endothelial cells (HUVEC) were obtained from the American Type Culture Collection. HUVEC were maintained in endothelial cell basal medium-2 (Cambrex Bio Science), as previously described (14).

Cell proliferation assay. All neuroblastoma cell lines were plated in 96-well plates (at 3-8 $\times$ 10^3 per well) in complete medium and cultured for 24 h. HUVEC were plated in 96-well plates (at 3 $\times$ 10^3 per well) precoated with collagen and then cultured for 24 h. The medium was removed and replaced with fresh complete medium that had been supplemented with different concentrations of either vinblastine (0-4 nmol/L) or rapamycin (0-100 nmol/L), alone or in combination for an additional 72 h. Cells were then pulse-labeled for 18 h with 0.5 μCi (0.0185 MBq) ^{3}H-thymidine (Amersham Biosciences), as previously described (25). Cell proliferation was tested by measuring DNA synthesis as a function of ^{3}H-thymidine uptake.

We further assessed if the association of the two drugs could have produced synergistic effects by calculating the combination indexes. Combination indexes were calculated as follow: CI_x = (D_1 combined / D_1 alone) + (D_2 combined / D_2 alone) + [(D_1 combined $\times$ D_2 combined) / (D_1 alone $\times$ D_2 alone)], where D_1 combined and D_2 combined represent the amount of drug 1 and drug 2, respectively, that caused 50% inhibition of cell growth. Both D_1 and D_2 alone displayed 50% inhibition for the mutually exclusive case where both drugs had different modes of action.

Analysis of DNA synthesis by pulse labeling with bromodeoxyuridine. Exponentially growing neuroblastoma cells (SH-SY5Y and GI-LI-N; 1.5-3 $\times$ 10^6 per 25-cm^2 flask) were treated for 24 h with either 1 or 2 nmol/L vinblastine (GI-LI-N and SH-SY5Y, respectively) and 10 nmol/L rapamycin, given alone or in combination. At the end of the treatment, cells were pulse-labeled with 10 μmol/L bromodeoxyuridine (BrdUrd; Sigma) for 30 min, as previously described (16). BrdUrd uptake was detected by staining the cells with 20 μL FITC-conjugated mouse monoclonal anti-BrdUrd antibody (Becton Dickinson) at a final concentration of 5 μg/mL for 30 min at room temperature. The cells were washed and resuspended in PBS containing 5 μg/mL propidium iodide. Bivariate distributions of BrdUrd amounts (FITC) versus DNA content (propidium iodide) were assessed by flow cytometry using a FACSCalibur device (Becton Dickinson), as previously described (16, 26). The gates represent the different phases of the cell cycle (R1, sub-G_1 phase; R2, G_1 phase; R3, S phase; R4, G_2-M phase).

Cell viability assay. Neuroblastoma cells (SH-SY5Y and GI-LI-N) were plated in 12-well plates (1.8-2.5 $\times$ 10^5 per well) and treated for 24 h as described above. Then, cells were harvested, washed with complete medium, and incubated with trypan blue (0.04%; Sigma), as previously described (26). The proportion of dead (or living) cells was calculated by dividing the number of dead (or living) cells by the total number of cells per field.

Phosphatidylserine detection. Phosphatidylserine exposure was assessed with a human Annexin V-FITC kit (Bender MedSystems). Briefly, cultured neuroblastoma cells (GI-LI-N and SH-SY5Y) were treated with vinblastine and rapamycin, administered alone or in combination as already mentioned in the previous paragraphs. Cells were then collected, washed, and incubated for 10 min with 5 μL Annexin V-FITC; washed once with PBS; resuspended in 190 μL prediluted binding buffer plus 10 μL of a 20 μg/mL propidium iodide stock solution; and examined by two-color flow cytometry using a FACSCalibur device, as described (16, 26).

Western blot analysis. Protein lysates were prepared, as previously described (26), from GI-LI-N and SH-SY5Y cells treated for 24 h with 1 nmol/L vinblastine (GI-LI-N), 2 nmol/L vinblastine (SH-SY5Y), and 10 nmol/L rapamycin, either alone or in combination. The protein lysates (40 μg per lane) were resolved on SDS/8% polyacrylamide gels; pre-stained molecular weight markers were run in parallel on each gel. The resolved proteins were transferred to nitrocellulose membranes; the membranes were then incubated with a rabbit monoclonal anti–phosphorylated p70 S6 kinase antibody (Thr^{389}; Upstate). The rabbit monoclonal anti–p70 S6 kinase antibody (Upstate) was used as a loading and transfer control. Peroxidase-conjugated goat anti-rabbit antibodies were used as secondary antibodies (Upstate and Chemicon International, respectively). Immune complexes were visualized with the use of an enhanced chemiluminescence system (Amersham International) according to the manufacturer's instructions.

Flow cytometry evaluation of vascular endothelial growth factor receptor 2. Neuroblastoma cells (ACN, SH-SY5Y, HTLA-230, and GI-LI-N) were plated in six-well plates (3-7.5 $\times$ 10^5 per well). The day after plating, neuroblastoma cells were treated for 24 h with 1 nmol/L vinblastine and 10 nmol/L rapamycin, administered alone or in combination. Cells were then collected by scraping and centrifuged at 1,100 rpm for 8 min. Thus, cells were processed for flow cytometry analysis. Briefly, 5 $\times$ 10^5 cells per point were incubated for 30 min at 4°C with an anti–vascular endothelial growth factor receptor 2 (VEGF-R2) mouse monoclonal antibody (clone ab9530, Abcam) at a concentration of 10 μg/mL. As negative control, cells were incubated with an isotype-matched monoclonal antibody (monoclonal mouse IgG1, Ancell Corp.). After incubation, cells were washed twice with 1% fetal bovine serum in PBS and then stained at 4°C for 20 min with a

FITC-conjugated goat anti-mouse immunoglobulin (Caltag Laboratories). After washing, cells that stained positive for VEGF-R2 were assessed by a FACSCalibur device, using Cell Quest Software. VEGF-R2 expression has been indicated as mean ratio fluorescence intensity, defined as the ratio between the fluorescence intensity of untreated and treated cells and the fluorescence intensity of their isotype-matched control antibody.

Quantitative evaluation of VEGF production. Neuroblastoma cells (ACN, SH-SY5Y, HTLA-230, and GI-LI-N) were plated and treated as described in the previous paragraph. Supernatants derived from each treatment point were then collected, sequentially centrifuged at 3,000 and 15,000 × *g* for 10 min, and stored at -80°C until use, as previously reported (27). Secretion of VEGF, by neuroblastoma cells, was determined using a human VEGF detection ELISA kit (R&D Systems GmbH), according to manufacturer's instruction. Because of the possible cytotoxic effects of vinblastine and rapamycin on these cells, the raw data obtained for VEGF concentrations were normalized for the number of viable cells.

In vivo *therapeutic studies in mice.* All experiments involving animals were reviewed and approved by the licensing and ethical committee of the National Cancer Research Institute, Genoa, Italy and by the Italian Ministry of Health. All *in vivo* experiments were done using eight mice per group and were repeated twice.

For these studies, we settled a very aggressive orthotopic neuroblastoma mouse model. Four-week-old female athymic (Nude-nu) mice were purchased from Harlan Laboratories and housed under specific pathogen-free conditions. Mice were anesthetized with ketamine (Imalgene 1000, Merial Italia S.p.A.), subjected to laparotomy, and injected with GI-LI-N cells (1.5×10^6 cells in 15 μL of saline solution) in the capsule of the left adrenal gland, as described (28, 29). No mice died as a result of this treatment. Tumors were allowed to grow from the injected cells for 14 days. At this time, mice were randomly assigned to four groups and treated with vinblastine and rapamycin, given alone or in combination. Rapamycin (1.5 mg/kg) was administered i.p. five consecutive days per week; vinblastine (0.5 mg/kg) was injected i.p. every 3 days. For the combined treatment, vinblastine and rapamycin were admixed together and injected as a single bolus. Treatment continued for a total of 5 weeks. Body weight and general physical status of the animals were recorded daily, and mice were killed by cervical dislocation after being anesthetized with xilezine (Xilor 2%, Bio98 Srl), when they showed signs of poor health, such as abdominal dilation, dehydration, or paraplegia.

Survival time, defined as the time (in days) between tumor cell inoculation and euthanasia of mice (n = 8 per group) due to evidence of poor health, was used as the main criterion for determining treatment efficacy. Measurement of tumor volumes has been even used as further confirmation of treatment efficacy. At various times after cell inoculation, mice (n = 3 per time; total, n = 18 per group) were randomly selected and killed by cervical dislocation after being anesthetized with xilezine, and their tumors were measured with calipers. Tumor volumes were calculated using the formula $\pi/6\ [w_1 \times (w_2)^2]$, where w_1 represents the largest tumor diameter, and w_2 represents the smallest tumor diameter.

Histologic analysis of mouse orthotopic tumors. Histologic evaluation of primary tumors was done 30 days after the beginning of the treatment. Briefly, orthotopic tumor-bearing mice (two mice per group) were anesthetized with xilezine and killed by cervical dislocation. Tumor masses were collected, split in two samples, and then processed for either paraffin or optimum cutting temperature compound (Miles Chemical Co.) embedding, respectively, as previously described (26).

Tissue sections (5 μm thick) were examined after staining with Mayer's H&E (Sigma Chemical Co.). Paraffin-embedded tissue sections were deparaffinized by the xylene-ethanol sequence, rehydrated in a graded ethanol scale and in TBS (pH 7.6), and then processed for antigen retrieval using a microwave, by boiling tissue sections in 0.1 mol/L EDTA (pH 8) for 10 min. The sections were then washed twice in PBS and saturated with 2% bovine serum albumin in PBS before staining with primary antibodies against CD31 that recognize endothelial cells (goat anti-mouse, clone SC-1506, Santa Cruz Biotechnology); the proliferation antigen Ki-67 (mouse anti-human Ki-67, clone MIB-1, DAKO); the endothelial cell marker CD34 (rat anti-mouse, clone MEC 14.7, DAKO); the 57-kDa human neuroblastoma-specific antigen, NB84a (mouse anti-human neuroblastoma, clone NB84a, DAKO); the VEGF (mouse anti-human VEGF, clone 26503, R&D Systems); the endothelial growth factor receptor 2 (mouse anti-human VEGF-R2, clone 89115, R&D Systems); and for terminal deoxynucleotidyl transferase–mediated nick-end labeling (TUNEL) analysis using the *In situ* Cell Death Detection kit (Roche), according to manufacturer's instructions. Binding of the primary antibodies was detected with horseradish peroxidase–conjugated horse anti-goat immunoglobulin G (Vector Laboratories) for immunohistochemical analysis and red phycoerythrin-conjugated rabbit anti-mouse (DAKO) or goat-anti-rat (Southern Biotech) or green FITC-conjugated goat anti-mouse (Caltag Laboratories) immunoglobulin for immunofluorescence analysis. Sections were analyzed for CD31 positivity by staining with diaminobenzidine substrate and, simultaneously, for apoptosis and for staining with the primary antibodies with a Nikon E-1000 fluorescence microscope equipped with specific filters for FITC, tetramethyl rhodamine isothiocyanate, and 4′,6-diamidino-2-phenylindole, as described (26, 30).

For VEGF and VEGF-R2 quantification, sections were observed under an Olympus photomicroscope (Olympus Italia) equipped for fluorescence and digital images acquisition. The intensity of VEGF- and VEGFR-2–related immunofluorescence (FITC label) from each section was quantified using the Image Analysis software (Olympus Italia). Red, green, and black images were obtained decomposing each original section, and the size of FITC-fluorescence brightness was determined by an accurate "thresholding" procedure on the green images. The results were expressed as percentage of FITC-labeled area referred to total area of the section.

Relative quantitative expression analysis of VEGF and VEGF-R2 in adrenal neuroblastoma xenograft in nude mice. Total RNA was isolated from tumor samples of adrenal neuroblastoma xenograft in nude mice, untreated and treated with rapamycin, vinblastine, or rapamycin + vinblastine, using the RNeasy Mini kit (QIAGEN) with an on-column DNase treatment. The concentration and quality control of all RNAs were assessed with the Agilent 2100 BioAnalyzer (Agilent Technologies). Expression analysis was done by a two-step reverse transcription-PCR. The first-strand cDNA was obtained by reverse transcription of 5 μg total RNA using a random primer-based synthesis (High-Capacity cDNA Archive kit, Applied Biosystems) according to the manufacturer's instructions. Relative quantitative expression analysis was carried out by duplex real-time reverse transcription-PCR using FAM-labeled Taqman Gene Expression Assays for each target gene (*VEGF* and *VEGF-R2*) and a VIC-labeled assay for the human *18S rRNA* housekeeping gene as endogenous control (reference gene), which resulted to be homogeneously and uniformly expressed in series of neuroblastoma cell lines and tumors from patients in a preliminary analysis.[5] Quadruplicates of each cDNA sample (25 ng) were amplified in the ABI 7700 PCR system (Applied Biosystems) according to the manufacturer's conditions and instructions. A validation assay was done to calculate PCR amplification efficiencies and construct a standard curve for each target gene (*VEGF* and *VEGF-R2*) and the housekeeping gene (*18S rRNA*) using serial dilutions of a given sample. Once the efficiency of target amplification was assessed to be similar to the reference one, the comparative C_t method or $\Delta\Delta C_t$ method was adopted for relative quantification of the target gene expression in tumor samples derived from untreated and treated mice as described (Applied Biosystems User Bulletin 2;[6] C_t, threshold cycle; i.e., the cycle at which the PCR reaction reaches a fluorescent intensity above background). After normalizing the C_t

[5] Patrizia Perri, personal communication.

[6] http://www.appliedbiosystems.com

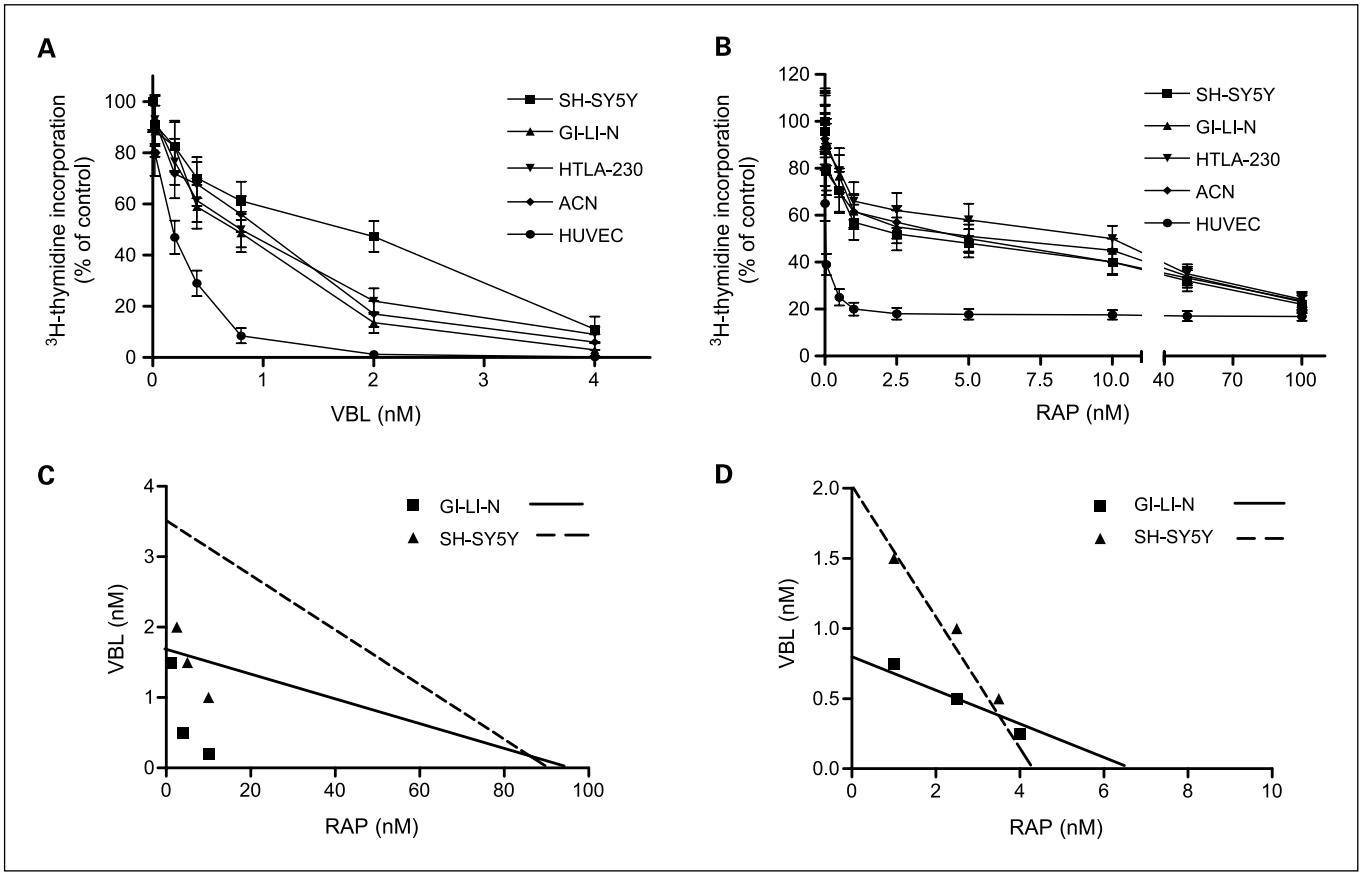

Fig. 1. Antiproliferative effects exhibited by vinblastine (*VBL*) and rapamycin (*RAP*) on neuroblastoma cell lines and HUVEC. Four neuroblastoma cell lines and HUVEC were cultured in the presence of various concentrations of either vinblastine (0-4 nmol/L) or rapamycin (0-100 nmol/L). Cell proliferation has been evaluated by ^{3}H-thymidine incorporation in quadruplicate wells. Points, mean percentage of ^{3}H-thymidine incorporation from quadruplicate wells compared with that of control untreated cells (*A* and *B*) from three different experiments; bars, SD. *C* and *D,* isobologram curves calculated for doses association of vinblastine and rapamycin that caused an inhibition of cell proliferation of 75% and 50%, respectively.

values of each target gene with the reference gene *18S rRNA* values (ΔC_t or mean normalized gene expression), we calibrated the normalized data with the control represented by an untreated tumor ($\Delta\Delta C_t$ or mean normalized expression relative to calibrator). Relative quantification of *VEGF* and *VEGF-R2* transcript levels is reported in Supplementary Fig. S3 as relative expression (%) observed in tumor samples treated with rapamycin, vinblastine, or rapamycin + vinblastine when compared with the control expression (calibrator), which has been set at 100.

Microvessel area. Microvessel area in tumor sections that were stained with the CD31 antibody was assessed independently by two investigators (B.N. and D.R.) with the use of a Quantimet 5000 computerized image analysis system (Leica), as previously described (26, 30).

Patients and collection of tumor samples. Ten neuroblastoma specimens collected from 1987 to 1998 were retrieved from the Italian Neuroblastoma Tissue Bank at the onset of the Ethical Committee of the G. Gaslini Children's Hospital, and all patients or their parents gave informed consent. Tumor cell content was always ≥80%. Disease extension was classified according to the International Neuroblastoma Staging System criteria (31). The specimens were from seven patients with stage IV, two patients with stage I, and one with localized stage II tumors.

Chick embryo chorioallantoic membrane assay. Chick embryo chorioallantoic membrane assays have been done according to Ribatti et al. (32). Briefly, growing chorioallantoic membranes (10 eggs per group) were treated by (*a*) overlaying them with 1-mm^3 sterilized gelatin sponges (Gelfoam Upjohn) that had been loaded with 1 μL PBS (negative control), 1 μL PBS containing 500 ng of recombinant fibroblast growth factor-2 (R&D Systems; positive control); (*b*) grafting fresh biopsy specimens from patients with neuroblastoma that had been collected under sterile conditions and minced in RPMI 1640 to obtain 1- to 2-mm^3 fragments onto the chorioallantoic membrane and then treated with PBS or 2 pmol/L vinblastine and 5 pmol/L rapamycin singly or in combination. These doses have been chosen based on our previous findings (16). The chorioallantoic membranes were examined daily until day 12 of incubation and then processed for light microscopy (26, 32). The angiogenic response was assessed by using a planimetric method of point counting (33). Mean values for microvessel area, with 95% confidence intervals (95% CI), were determined for each analysis.

Statistical analysis. All *in vitro* data are from at least three independent experiments, and the results are expressed as mean values with SD. To determine whether drug combinations exhibited synergistic antiproliferative activity, isobolographic analysis was done. From the dose-response curves, the concentration at which neuroblastoma cell proliferation was inhibited to 75% and to 50% of control level was calculated to generate the isobolograms. The diagonal line shows the theoretical line indicating additive effects: the points below the line indicate synergistic activity, whereas those above the line represent subadditivity. Different combinations of vinblastine and rapamycin were added to neuroblastoma cells, and the values obtained were plotted in the isobolograms.

The statistical significance of differences between experimental and control groups was determined by ANOVA with Tukey's multiple comparison test using GraphPad Prism 3.0 software (GraphPad

Software, Inc.). Survival curves were constructed by using the Kaplan-Meier method. All *in vivo* experiments were done twice with similar results, and the data are expressed as mean values with 95% CI. Survival in different treatment groups was compared by using Peto's log-rank test in StatsDirect 0.1 statistical software (CamCode). All statistical tests were two sided, and $P < 0.05$ was considered statistically significant.

Results

Combined treatment with vinblastine and rapamycin inhibits neuroblastoma cell proliferation. We investigated the antiproliferative effects of vinblastine and rapamycin on four neuroblastoma cell lines and HUVEC *in vitro*, by measuring ^{3}H-thymidine uptake. Both drugs showed a dose-dependent inhibition of cell proliferation on all neuroblastoma cell lines examined as well as on endothelial cells, after a 72-h treatment (Fig. 1A and B). The dose-response curves plotted in Fig. 1 showed that HUVEC were more sensitive to vinblastine and rapamycin (drug concentration that caused IC_{50} = 200 pmol/L for vinblastine and 75 pmol/L for rapamycin), with respect to neuroblastoma cells (mean IC_{50} = 1.1 $\pm$ 0.4 nmol/L for vinblastine and mean IC_{50} = 5.5 $\pm$ 2 nmol/L for rapamycin).

In our previous report (16), we observed that vinblastine and rapamycin produced, on endothelial cells, a synergistic antiproliferative effect, defined as a combination of two drugs, showing a greater efficacy than that of the expected sum of the effects of each drug.

To determine whether vinblastine and rapamycin in combination had synergistic activity also on neuroblastoma cells, different combinations of concentrations of vinblastine and rapamycin were added to neuroblastoma cells. From the dose-response curves, the concentrations at which GI-LI-N and SH-SY5Y cells proliferation was inhibited to 75% and to 50% of control were calculated. Figure 1C and D shows the isobolograms generated from these data, respectively. When compared with the theoretical line representing additive effect, only the values from the combination treatment obtained at the IC_{75} fall below the line indicating synergistic activity for this end point, whereas their effects likely indicated summation when combined to reach a 50% inhibition of cell growth. Similar results have been obtained also for HTLA-230 and ACN cells (data not shown). Nevertheless, the combined treatment produced, on HUVEC, synergistic antiproliferative effects at both IC_{75} and IC_{50}, as expected from our previous work (16).

To have proof-of-principle data regarding the efficacy of the doses herein used of rapamycin alone or in combination with vinblastine on neuroblastoma cells, Western blot analysis has been done on cells treated with these drugs, and S6K protein expression was evaluated. P-S6K (Thr^{389}) was found to be constitutively expressed in neuroblastoma cells, and rapamycin alone and in combination with vinblastine was found to suppress phosphorylated S6K levels, without affecting S6K protein levels (Supplementary Fig. S1).

Vinblastine and rapamycin induce cell cycle arrest in neuroblastoma cells. To investigate whether the antiproliferative effect, displayed by the combination of vinblastine and rapamycin, was associated to an inhibition of cell cycle progression, SH-SY5Y and GI-LI-N cells were treated for 24 h

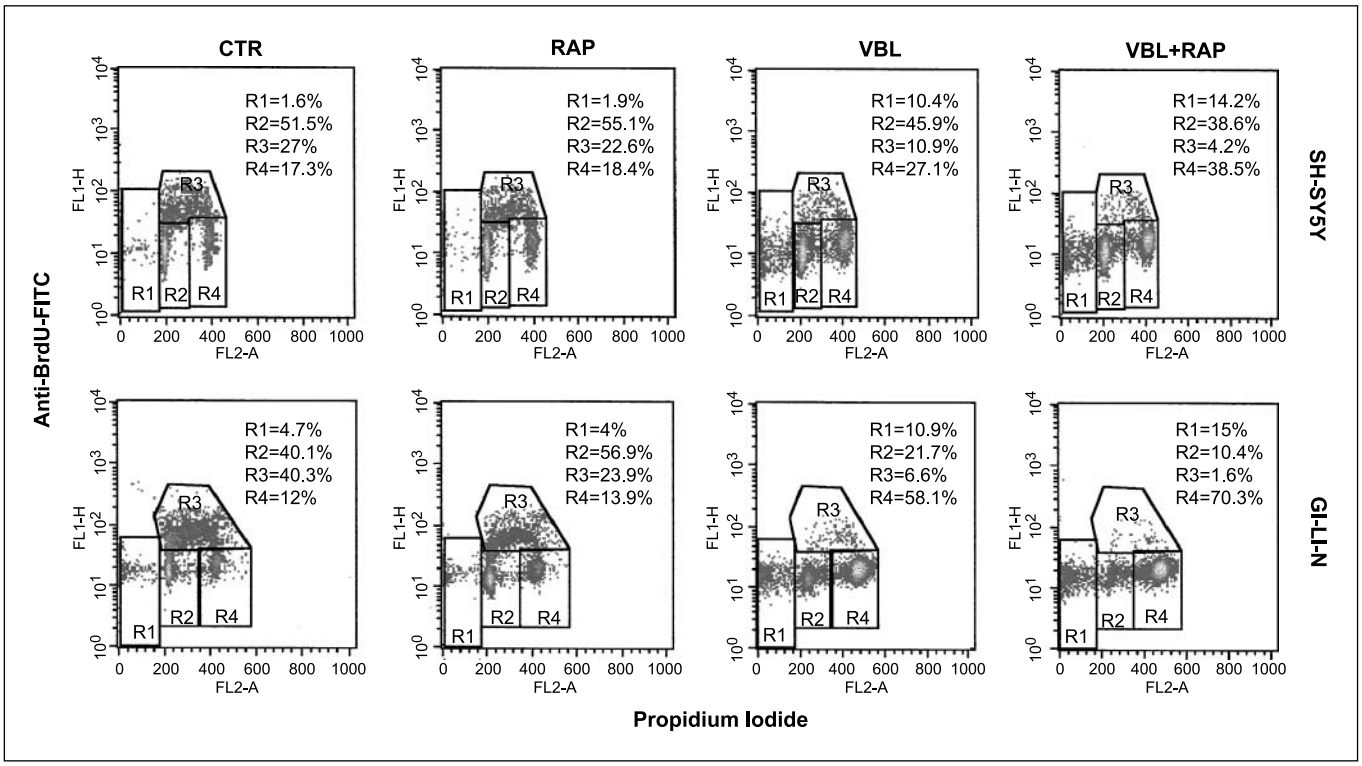

Fig. 2. Effect of vinblastine and rapamycin on neuroblastoma cell cycle progression. SH-SY5Y and GI-LI-N cells were exposed to either 2 or 1 nmol/L vinblastine, respectively, and 10 nmol/L rapamycin, given alone or in combination, for a total of 24 h. Cells were then analyzed for DNA synthesis by pulse labeling with BrdUrd. BrdUrd uptake (FITC, *Y*-axis) versus total cellular DNA content (propidium iodide, *X*-axis) was evaluated by densitometric fluorescence activated cell sorter analysis. The gates represent the different phases of the cell cycle (R1, sub-G_1 phase; R2, G_1 phase; R3, S phase; R4, G_2-M phase).

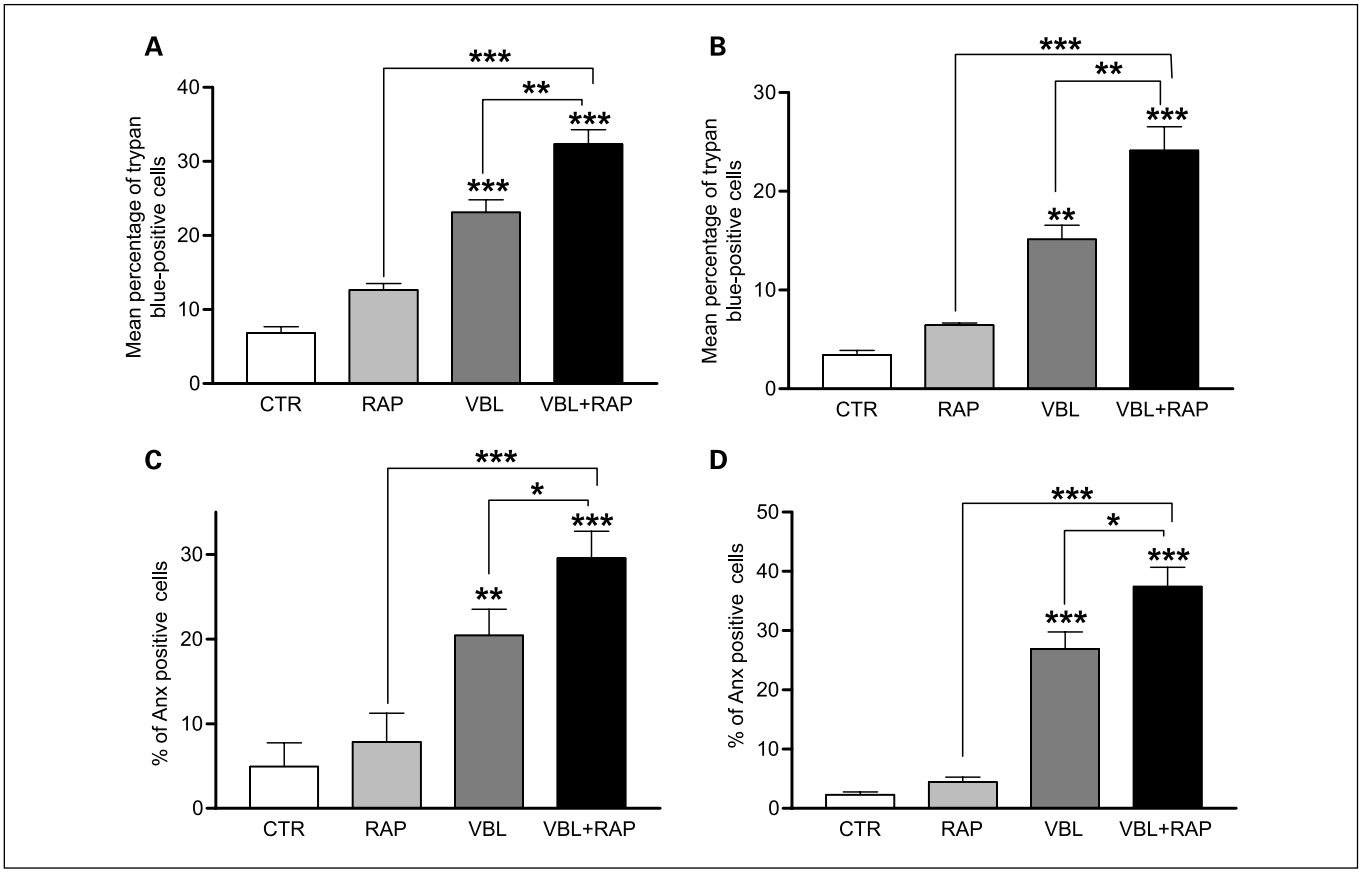

Fig. 3. Vinblastine and rapamycin induce cell death in human neuroblastoma cell lines. GI-LI-N (*A* and *C*) and SH-SY5Y (*B* and *D*) were treated with either 1 nmol/L (GI-LI-N) or 2 nmol/L vinblastine (SH-SY5Y) and 10 nmol/L rapamycin, administered separately or together, for 24 h. *A* and *B,* cell death induction, as assessed by trypan blue staining. *C* and *D,* apoptosis induction, determined as the percentage of Annexin-positive cells. Columns, mean; bars, SD. **, $P < 0.01$; ***, $P < 0.001$ versus control, calculated using ANOVA with Tukey's multiple comparison test.

with either 2 or 1 nmol/L vinblastine, respectively, and 10 nmol/L rapamycin, given alone or in combination. These drug concentrations were chosen because they represent likely the IC_{50} on the two cell lines. Cells were then pulse-labeled with BrdUrd to examine DNA synthesis. BrdUrd uptake versus total cellular DNA content was then evaluated by densitometric fluorescence-activated cell sorting analysis.

As shown in Fig. 2, treatment with rapamycin alone induced, as expected, a G_1 phase cell cycle arrest (R2), in both neuroblastoma cell lines analyzed. Vinblastine treatment led to a marked G_2-M phase cell cycle arrest (R_4), associated with a pronounced decrease of cells actively synthesizing DNA (R_3). Furthermore, the combined treatment resulted in a more dramatic block of neuroblastoma cells in G_2-M phase [vinblastine, 56 ± 5% of GI-LI-N cells in G_2-M phase; rapamycin, 15 ± 2%; vinblastine + rapamycin, 69 ± 6% ($P < 0.05$ and $P < 0.001$ versus vinblastine and rapamycin, respectively); vinblastine, 26 ± 3% of SH-SY5Y cells in G_2-M phase; rapamycin, 19.5 ± 2%; vinblastine + rapamycin, 39.9 ± 4% ($P < 0.001$ and $P < 0.001$ versus vinblastine and rapamycin, respectively)] and a complete arrest of the S phase [vinblastine, 7.2 ± 0.75% of GI-LI-N cells in S phase; rapamycin, 24.5 ± 3%; vinblastine + rapamycin, 1.5 ± 0.2% ($P < 0.05$ and $P < 0.001$ versus vinblastine and rapamycin, respectively); vinblastine, 12.9 ± 1.5% of SH-SY5Y cells in S phase; rapamycin, 21.7 ± 2.3%; vinblastine + rapamycin, 4 ± 0.3% ($P < 0.01$ and $P < 0.001$ versus vinblastine and rapamycin, respectively)], suggesting that when used together, the two drugs, work to increase the effect produced by vinblastine given alone. These results could explain the dramatic antiproliferative effects produced by the combined treatment with vinblastine and rapamycin.

Vinblastine and rapamycin lead to an induction of cell death in neuroblastoma cells. Next, we investigated the effects of vinblastine and rapamycin on SH-SY5Y and GI-LI-N cells, through the evaluation of cell death induction. Neuroblastoma cells were treated for 24 h with either 1 nmol/L (GI-LI-N) or 2 nmol/L vinblastine (SH-SY5Y) and 10 nmol/L rapamycin, delivered alone or in combination. At the end of the treatment, cells were collected and analyzed for both cell viability (trypan blue assay) and apoptosis (phosphatidylserine detection assay).

As shown in Fig. 3A and B, rapamycin produced an induction of cell death, with respect to control cells, even if not statistically significant. On the other hand, vinblastine treatment resulted in a statistically significant induction of cell death, on both cell lines examined (GI-LI-N, *A*; SH-SY5Y, *B*), with a further significant increase of trypan blue–positive cells caused by the combined treatment (**, $P < 0.01$, vinblastine + rapamycin versus vinblastine; ***, $P < 0.001$, vinblastine + rapamycin versus rapamycin).

In subsequent experiments, we investigated whether the observed cell death could be due to apoptosis induction. Phosphatidylserine exposure detection assays showed that,

similarly to the results obtained in the aforementioned cell viability experiments, treatment with rapamycin had a slight proapoptotic effect. In contrast, after vinblastine treatment, we observed a statistically significant increase in the percentage of Annexin-positive cells that was significantly enhanced by the two drugs used in combination (Fig. 3C and D: *, $P < 0.05$, vinblastine + rapamycin versus vinblastine; ***, $P < 0.001$, vinblastine + rapamycin versus rapamycin). These results suggest that the vinblastine and rapamycin induced cell death could be due to apoptosis.

Combined therapeutic effects of vinblastine and rapamycin in human neuroblastoma orthotopic mouse model. To investigate whether the combined treatment with vinblastine and rapamycin could have antitumor effectiveness against human neuroblastoma *in vivo*, we settled an aggressive and highly angiogenic orthotopic mouse model by injecting GI-LI-N cells in the adrenal gland of nude mice. Different criteria were adopted to evaluate the therapeutic efficacy of our treatments. First, we assessed the antitumor effect produced by both the drugs, used alone or in combination, in terms of inhibition of tumor growth. As reported in Fig. 4A, at 30 days after the beginning of the treatment, mice treated with vinblastine and rapamycin, given alone, had statistically significant smaller primary tumor masses than control mice [mean tumor volume of vinblastine-treated versus untreated group: 503 versus 2,200 mm^3 (difference, 1,697 mm^3; 95% CI, 1,344-2,050 mm^3), $P < 0.001$; mean tumor volume of rapamycin-treated versus untreated group: 553 versus 2,200 mm^3 (difference, 1,647 mm^3; 95% CI, 1,294-2,000 mm^3), $P < 0.001$]. Noteworthy, mice treated with the combination of the two drugs had even smaller tumor masses [mean tumor volume of vinblastine + rapamycin-treated versus untreated group: 218 versus 2,200 mm^3 (difference, 1,982 mm^3; 95% CI, 1,629-2,335 mm^3), $P < 0.001$]. Moreover, at 50 days after start of treatment, when all of control mice had died, the volumes of primary tumor masses from mice treated with the drug combination were statistically smaller than those of tumors from mice treated with either drug administered separately [mean tumor volume of vinblastine + rapamycin-treated versus rapamycin-treated group: 280 versus 810 mm^3 (difference, 530 mm^3; 95% CI, 323.7-736.3 mm^3), $P < 0.001$; mean tumor volume of vinblastine + rapamycin-treated versus vinblastine-treated group: 280 versus 980 mm^3 (difference, 700 mm^3; 95% CI, 493.7-906.3 mm^3), $P < 0.001$]. A further evidence, for the efficacy of our treatments, came from the count of CD31-positive blood vessels within primary tumor masses of treated mice. Figure 4B shows that vinblastine treatment led to a statistically significant decrease of CD31-positive blood vessels,

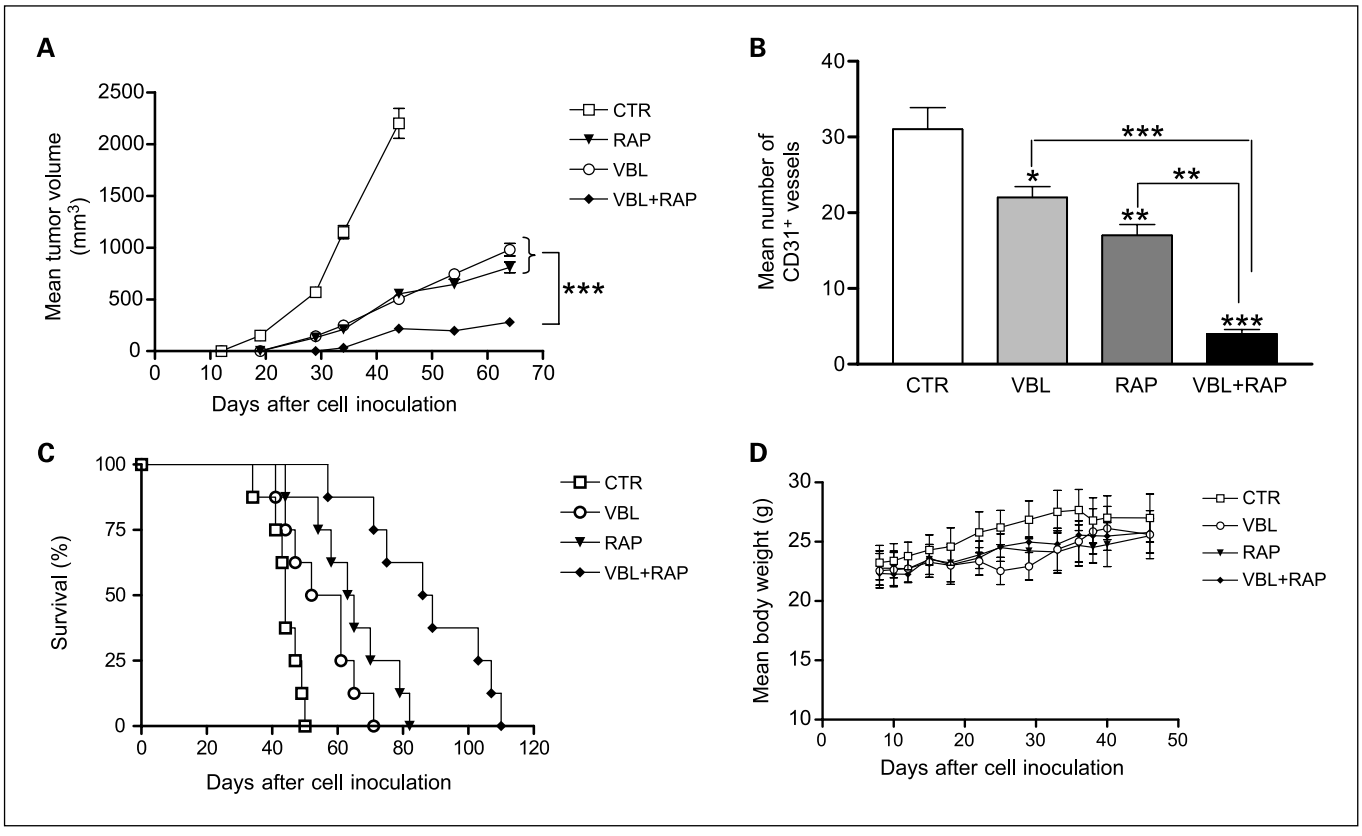

Fig. 4. *In vivo* antitumor effectiveness of vinblastine and rapamycin. Nude mice were orthotopically injected with GI-LI-N cells, and tumors were allowed to growth for 14 d. At that time, mice were randomly assigned to four groups and treated with saline (control), rapamycin (1.5 mg/kg), vinblastine (0.5 mg/kg), or vinblastine + rapamycin at the same doses used separately. *A,* the therapeutic efficacy of treatments was determined as function of tumor growth inhibition. Tumor volumes were measured as described in Materials and Methods. The difference between control and treated mice were analyzed by ANOVA with Tukey's multiple comparison test. ***, $P < 0.001$. *B,* the change in the mean number of CD31-positive blood vessels was evaluated on tumor masses excised from neuroblastoma-bearing mice, 30 d after the beginning of the treatment. Columns, mean; bars, 95% CI. *, $P < 0.05$; **, $P < 0.01$; ***, $P < 0.001$ versus control, calculated using ANOVA with Tukey's multiple comparison test. *C,* survival of mice was monitored daily and used as criterion to evaluate the therapeutic effectiveness of treatments. Survival curves were compared by using Peto's log-rank test. *D,* mice body weight changes were recorded and used to monitor drug-induced toxicity.

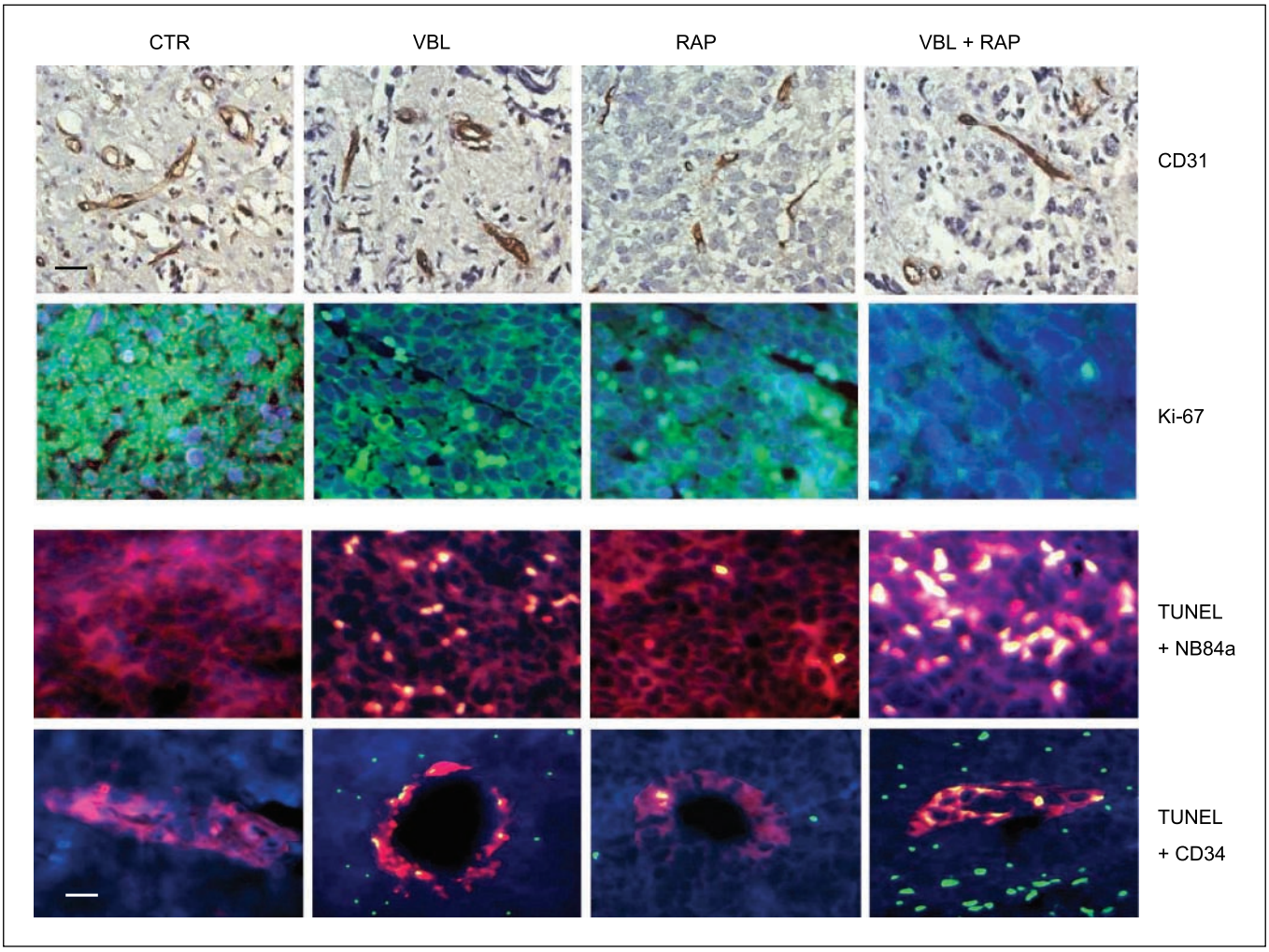

Fig. 5. Immunohistochemical and immunofluorescence analysis of primary tumor masses derived from untreated or vinblastine- and rapamycin-treated mice. Tumor masses were excised on day 30 from the beginning of the treatment and then stained for CD31 (to show blood vessels; bar, 200 μm); for the cell proliferation marker Ki-67; for NB84a, neuroblastoma-specific antigen and apoptosis (NB84a + TUNEL); for the specific endothelial cell marker CD34 and apoptosis (CD34 + TUNEL). Brown, CD31-positive blood vessels; green, Ki-67 – positive cells orTUNEL-positive cells; red, NB84a-positive neuroblastoma cells or CD34-positive endothelial cells; yellow, colocalization of TUNEL-positive/NB84a-positive neuroblastoma cells orTUNEL-positive/CD34-positive endothelial cells. Cell nuclei were stained with 4′,6-diamidino-2-phenylindole (*blue*). Bar, 100 μm.

with respect to control; this reduction was even more significant in tumor masses derived from mice treated with rapamycin. Finally, the combined treatment caused the maximum decrease of blood vessel count that was statistically different from the single drugs (**, $P < 0.01$, vinblastine + rapamycin versus rapamycin; ***, $P < 0.001$, vinblastine + rapamycin versus vinblastine).

As a second criterion to evaluate the therapeutic effectiveness of our treatments, we used the survival time of treated mice. Both the drugs administered alone triggered to a statistically significant increase in life span, with respect to saline-injected control animals (vinblastine versus CTR, $P = 0.04$; rapamycin versus CTR, $P = 0.0015$). Moreover, the combined treatment led to a superior increase in life span that was statistically significant with respect to control mice (vinblastine + rapamycin versus CTR, $P = 0.0002$) and, noteworthy, statistically significant with respect to either vinblastine- or rapamycin-treated mice (vinblastine + rapamycin versus vinblastine, $P = 0.002$; vinblastine + rapamycin versus rapamycin, $P = 0.0162$).

Vinblastine and rapamycin, administered alone or in combination, gave only minimal side effects, as shown by recording of mice body weight (in grams) plotted in Fig. 4*D*.

***Combination therapy with vinblastine and rapamycin increases anti-vascular effects, tumor growth inhibition, and apoptosis* in vivo.** Once shown the therapeutic efficacy of the combined treatment against human neuroblastoma *in vivo*, we decided to elucidate the mechanisms responsible of the aforementioned effects. With this purpose, histologic and immunofluorescence experiments on paraffin-embedded tissue sections derived from orthotopic tumor-bearing mice have been done. As shown in Fig. 5, treatment with either vinblastine or rapamycin led to a destruction of tumor vasculature, evidenced by the lack of CD31 staining that was more evident in tissue sections derived from rapamycin-treated mice. Moreover, the combined treatment resulted in an almost complete loss of tumor blood vessels, in agreement with the results presented in Fig. 4B. The effect of our treatments was also very important in terms of inhibition of cell proliferation, as assessed by the detection

of Ki-67 antigen (Fig. 5). In this regard, tissue sections derived from mice treated with vinblastine and rapamycin, given alone, showed a marked inhibition of cell growth, with respect to control; the combined treatment showed once again the significant capability to almost completely arrest tumor cell proliferation. Indeed, the percentage of Ki-67–positive cells was also quantified in four random fields from two independent experiments: control, 87.5 ± 9.5% Ki-67$^+$ cells; vinblastine, 50 ± 7.5% ($P < 0.001$ versus control); rapamycin, 37.5 ± 5% ($P < 0.001$ versus control); vinblastine + rapamycin, 5.5 ± 1.5% ($P < 0.001$ versus control, $P < 0.001$ versus vinblastine, $P < 0.01$ versus rapamycin). Next, we investigated the potential of our combined treatment in terms of apoptosis induction. As shown in Fig. 5, tumors derived from mice treated with the combination of the two drugs presented a pronounced number of apoptotic cells, both neuroblastoma and endothelial cells, as assessed by the double staining with TUNEL plus NB84a and TUNEL plus CD34, respectively. These apoptotic features were clearly evident with respect to untreated mice and, statistically relevant, also compared with tumors derived from either vinblastine- or rapamycin-treated mice individually. Indeed, the percentage of TUNEL$^+$-NB84a$^+$ cells was quantified in four random fields from two independent experiments: control, 1 ± 1% TUNEL$^+$-NB84a$^+$ cells; vinblastine, 31.5 ± 5% ($P < 0.001$ versus control); rapamycin, 12 ± 3%; vinblastine + rapamycin, 51 ± 7.5% ($P < 0.001$ versus control, $P < 0.01$ versus vinblastine, $P < 0.001$ versus rapamycin). Finally, the percentage of TUNEL$^+$-CD34$^+$ cells was quantified in four random fields from two independent experiments: control, 1 ± 1% TUNEL$^+$-CD34$^+$ cells; vinblastine, 30 ± 4.5% ($P < 0.001$ versus control); rapamycin, 18 ± 3.5% ($P < 0.01$ versus control); vinblastine + rapamycin, 44 ± 5% ($P < 0.001$ versus control, $P < 0.01$ versus vinblastine, $P < 0.001$ versus rapamycin). Noteworthy, vinblastine + rapamycin–induced apoptosis was detected in tumor tissues but not in normal tissues, such as heart, lung, kidneys, liver, and spleen (data not shown).

Finally, we did histologic studies after only 1 week from the beginning of treatment, when the sizes of the tumors in the different branches were similar. The results presented in Supplementary Fig. S2 are superimposable to those presented in Fig. 5.

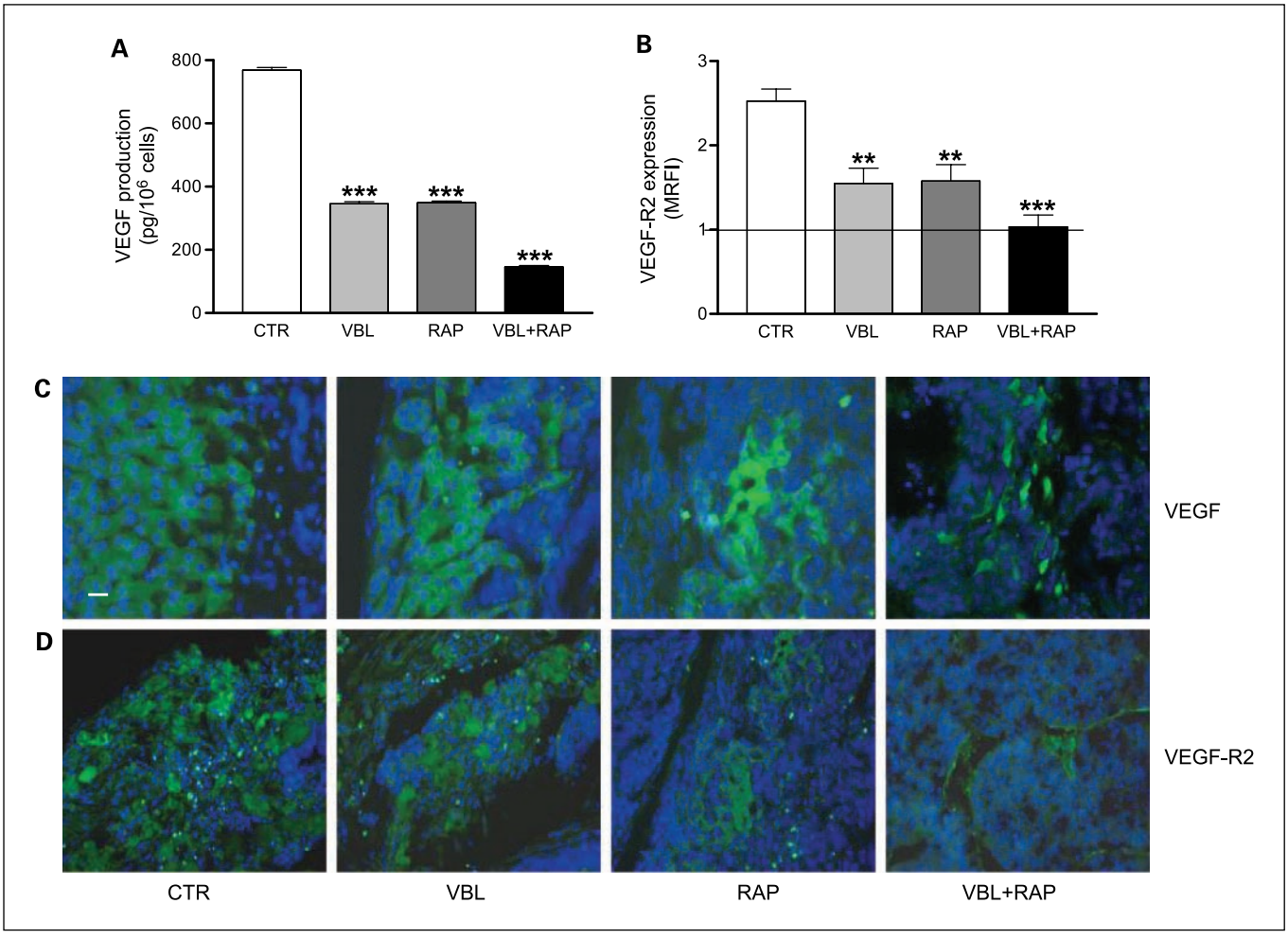

Fig. 6. Down-modulation of VEGF molecule production and VEGF-R2 expression on neuroblastoma. *A* and *B,* GI-LI-N cells were treated with 1 nmol/L vinblastine and 10 nmol/L rapamycin, alone or in combination for 24 h. Secretion of VEGF molecule was quantified, as described in Materials and Methods, in the cell culture supernatants derived from each treatment point. Columns, pg/10^6 cells; bars, SD (*A*). The expression of VEGF-R2 was evaluated on neuroblastoma cells, by flow cytometry. Columns, mean ratio fluorescence intensity (*MRFI*); bars, SD. Mean ratio fluorescence intensity of 1 indicate no antigen expression (*B*). **, $P < 0.01$; ***, $P < 0.001$ versus control, calculated using ANOVA with Tukey's multiple comparison test. *C* and *D,* tumor masses excised from neuroblastoma-bearing mice, on day 30 from the beginning of the treatment, were immunostained (*green*) for both VEGF (*C*) and VEGF-R2 (*D*). Cell nuclei were stained with 4′,6-diamidino-2-phenylindole (*blue*). Bar, 100 μm.

***Combined administration of vinblastine and rapamycin down-modulate VEGF and VEGF-R2* in vitro *and* in vivo.** Because we showed that part of the observed therapeutic effects, obtained through the combined treatment, depend, at least in part, on an antiangiogenic activity, we did experiments to investigate whether our treatment could also affect, *in vitro* and *in vivo*, the production of VEGF molecule, as well as modulate the expression of its receptor KDR (VEGF-R2), being the main proangiogenic loop involved in neuroblastoma-induced angiogenesis (13, 34, 35).

To this purpose, we determined the physiologic production of VEGF on a panel of neuroblastoma cells (SH-SY5Y, HTLA-230, GI-LI-N, and ACN). Although all the neuroblastoma cells analyzed produced VEGF, even if at different levels (data not shown), we focused our attention on GI-LI-N cells, being those chosen for the orthotopic *in vivo* model. Figure 6A shows that either vinblastine or rapamycin down-modulated significantly the production of VEGF, compared with control cells (2-fold reduction). Furthermore, the combined treatment caused a more evident decrease in the secretion of VEGF (roughly, a 4-fold decrease), with respect to control cells. To rule out the possibility that the decreased VEGF production could simply be a reflection of cytotoxicity of vinblastine and rapamycin, the raw data were normalized for the number of viable cells. Moreover, the apoptogenic drug Fenretinide was not able to consistently modulate VEGF production and secretion, confirming our previous findings (ref. 27; data not shown). In regard to the expression of VEGF-R2, two of four neuroblastoma cell lines analyzed (GI-LI-N and SH-SY5Y) expressed the receptor. Also in this case, we focused on GI-LI-N cells. As shown in Fig. 6B, either vinblastine or rapamycin treatment led to a statistically significant down-modulation of VEGF-R2 expression, compared with control cells. Noteworthy, the down-modulation became more statistically significant, reaching a complete switching off of receptor expression, when the cells were exposed to the combination of the two drugs. The relevance of these results has been further confirmed by *in vivo* assaying the effects of the combined treatment on VEGF and VEGF-R2 expression. In this case, tissue sections of primary tumor masses, derived from untreated or treated mice, were excised on day 25 from the beginning of the treatment and then stained for both VEGF (Fig. 6C) and VEGF-R2 (Fig. 6D) expression. As shown in Fig. 6C and D, either vinblastine or rapamycin induced a decrease of VEGF and VEGF-R2, more marked in primary masses excised from rapamycin-treated animals. Again, the simultaneous administration of both the drugs resulted in a stronger effect, leading to an almost complete disappearance of the aforementioned proangiogenic molecules. Indeed, the percentage of VEGF-positive cells were quantified in four random fields from two independent experiments: control, 58 $\pm$ 7.5% $VEGF^+$ cells; vinblastine, 44 $\pm$ 6% (not significant versus control); rapamycin, 25 $\pm$ 4.5% ($P < 0.01$ versus control); vinblastine + rapamycin, 12.5 $\pm$ 2.5% ($P < 0.001$ versus control, $P < 0.001$ versus vinblastine, $P < 0.01$ versus rapamycin). Moreover, the percentage of VEGF-R2–positive cells were quantified in four random fields from two independent experiments: control, 55 $\pm$ 7.5% $VEGF\text{-}R2^+$ cells; vinblastine, 35 $\pm$ 5.5% ($P < 0.05$ versus control); rapamycin, 18 $\pm$ 3% ($P < 0.001$ versus control); vinblastine + rapamycin, 3 $\pm$ 0.5% ($P < 0.001$ versus control, $P < 0.001$ versus vinblastine, $P < 0.01$ versus rapamycin).

To support the *in vivo* relevance of these findings, relative quantitative reverse transcription-PCR analysis has been also done on tumor samples derived from orthotopic-engrafted animals, untreated and treated with the various drugs for 1 week. In accordance to the *in vitro* (see Fig. 6A and B) and *in vivo* findings (Fig. 6C and D), both *VEGF* and *VEGF-R2* expression levels resulted to be down-regulated by either the single drugs or the combination of vinblastine + rapamycin (Supplementary Fig. S3).

Finally, to further rule out that the antitumor efficacy was only due to the effect on tumor vasculature, we did double staining also on *in vivo* VEGF and VEGF-R2 expression regulation. As clearly observed in Supplementary Fig. S4, both molecules were co-expressed on both endothelial and neuroblastoma cells and were down-regulated by the combination of vinblastine + rapamycin in both cells.

Taken together, these results seem to suggest that the therapeutic efficacy of the combined treatment could be explained through a double mechanism of action: the first one that directly affects tumor cells and the second one that causes damage to endothelial tumor cells, with consequent effects on cancer cells.

Combination therapy with vinblastine and rapamycin inhibits angiogenesis induced* in vivo *by human neuroblastoma biopsy specimens. Chick embryo chorioallantoic membrane assays were done to further assess the effectiveness of vinblastine and rapamycin in inhibiting angiogenesis *in vivo*. The morphometric evaluations of microvessel area were done on day 12 of incubation with the sponges or the neuroblastoma biopsies. Microscopic examination of the microvessel area of chorioallantoic membranes revealed highly vascularized tissue among the trabeculae of the sponges loaded with the positive control fibroblast growth factor-2 (3.30×10^{-2} mm^2; 95% CI, 2.5-4.4 $\times$ 10^{-2} mm^2) and those loaded with human neuroblastoma biopsy specimens alone (3.1×10^{-2} mm^2; 95% CI, 2.65-3.55 $\times$ 10^{-2} mm^2). Addition of vinblastine significantly reduced the microvessel area (1.75×10^{-2} mm^2; 95% CI, 1.45-2.1 $\times$ 10^{-2} mm^2; $P < 0.01$ versus biopsy specimens alone). Similar results were obtained even after addition of rapamycin (1.55×10^{-2} mm^2; 95% CI, 1.35-1.75 $\times$ 10^{-2} mm^2; $P < 0.01$ versus biopsy specimens alone). The two drugs used in combination displayed a significantly greater angiostatic activity (0.77×10^{-2} mm^2; 95% CI, 0.65-0.9 $\times$ 10^{-2} mm2; $P < 0.001$ versus biopsy specimens alone) then the single drugs ($P < 0.05$ versus vinblastine; $P < 0.05$ versus rapamycin). These results further confirm the implication of an antiangiogenic activity, concordant with our previous data (16), in the therapeutic efficacy of vinblastine and rapamycin.

Discussion

In this study, we have shown for the first time that vinblastine and rapamycin, used in combination, exhibit a greater antitumor effectiveness with respect to either drug used separately, *in vitro* against a panel of human neuroblastoma cell lines, and *in vivo* against a biologically and clinically relevant, highly angiogenic neuroblastoma mouse model.

One of the major goals in cancer research is to develop new therapeutic approaches having limited side effects and good efficacy. This aim is terribly pregnant in neuroblastoma research because, in spite of the application of aggressive

treatment strategies, the great outcome for this disease is quite poor (2). The rationale to use vinblastine and rapamycin in combination stems from three major reasons. First, vinblastine and rapamycin act by affecting cell cycle progression in different phases (4, 10); thus, the effects produced when used alone would, reasonably, lead to a greater result if used together. Second, it has been reported that the mammalian target of rapamycin inhibitor rapamycin sensitizes several tumor cells to chemotherapeutics (36, 37). Third, vinblastine and rapamycin are well-known drugs already used in clinical practice; thus, a new approach based on the combination of the two molecules could be easily transferred to clinical therapy.

Recently, we showed that vinblastine and rapamycin exerted synergistic inhibition of human neuroblastoma-related angiogenesis (16). Here, we found that combination of vinblastine and rapamycin resulted in a marked inhibition of neuroblastoma and endothelial cell growth, leading to a drastic antiproliferative result. The inhibition of cell proliferation induced by these two drugs has been associated to an impaired cell cycle progression in other tumor models (38, 39). Accordingly, our findings showed that also in neuroblastoma cells vinblastine and rapamycin, used together, triggered a dramatic G_2-M phase cell cycle arrest, coupled to an almost complete depletion of cells actively synthesizing DNA. This result suggests that the effect obtained by the single administration of vinblastine (G_2-M phase block) is likely increased through the addition of rapamycin, according to previous studies (40, 41) in which rapamycin was shown to enhance the efficacy of several chemotherapeutics.

Vinblastine and rapamycin used in combination led to a stronger cell death induction compared with that obtained by either drug tested alone. Furthermore, our data suggested that the observed cell death could be due to apoptosis, as already shown for the activity of vinblastine in other tumor cells (42). However, although our findings suggest that apoptosis activation has a role in vinblastine plus rapamycin triggered cell death, the upstream signals that lie between drug exposure and programmed cell death are still unknown as is whether mechanisms of cell death other than apoptosis, such as mitotic catastrophe and autophagy, are involved in the function of vinblastine plus rapamycin (43, 44). Nevertheless, our recent data (17) showed that the combined treatment of endothelial cells with vinblastine and rapamycin led to the modulation of molecules involved in the apoptotic pathway.

We observed that vinblastine and rapamycin, given in combination, inhibited neuroblastoma tumor growth and angiogenesis, leading to a statistically significant increased life span in mice orthotopically implanted with a highly angiogenic and *MYCN*-amplified human neuroblastoma cell line (35, 45). This model is biologically and clinically relevant, mimicking a condition of disease with primary tumor and disseminated metastases, similarly to our already described neuroblastoma orthotopic model (29) obtained by injecting the *MYCN* single copy neuroblastoma cell line SH-SY5Y, even if with a more aggressive metastatic spreading. The *MYCN*-amplified GI-LI-N cells have been chosen because of their highly angiogenic features; indeed, as previously reported by us (35), GI-LI-N cells present angiogenic behavior *in vitro* and *in vivo*. Furthermore, we have also shown that *in vivo* angiogenic activity of neuroblastoma correlates with *MYCN* oncogene overexpression (45). The aggressiveness and the metastatic spreading as well as the highly angiogenic properties of our orthotopic neuroblastoma mouse model gave us the opportunity to elucidate the mechanisms of action that underlie to the obtained therapeutic results. Immunohistochemical analyses of orthotopic neuroblastoma tumors showed a statistically significant decrease in microvessel density and cell proliferation, associated to an increase in apoptotic neuroblastoma and endothelial cells. The above data could be consistent with the hypothesis that the therapeutic efficacy of the combined treatment is due, at least in part, to an antiangiogenic effect, consistently with our previous findings (16). Through these results, we can postulate that the combined therapy works by a double mechanism of action. The first one that damages directly tumor cells by inhibiting tumor cell proliferation and inducing apoptosis; the second one that produces injuries to endothelial cells, with consequent effects on cancer cells. This conclusion is consistent with the concept that a strategy affecting both tumor vasculature and tumor cells themselves may be more efficacious (30, 46, 47) than approaches directed against only one of the two therapeutic targets.

Because we showed that antiangiogenesis had an important role in our therapeutic results, we investigated the potential effect of the combined treatment in the modulation of VEGF and its KDR receptor (VEGF-R2). Indeed, VEGF plays a critical role in tumor angiogenesis and is expressed in a number of human tumors (48, 49), including neuroblastoma (50). It has also been envisaged the possibility that VEGF could take part to neuroblastoma progression by directly regulating neuroblastoma cell growth (51). Interestingly, in neuroblastoma tumors, VEGF, as well as VEGF-R2, expression is associated with poor prognosis (34, 52). Here, we observed that the administration of vinblastine and rapamycin in combination produced a statistically significant decrease in the secretion of VEGF molecule, as well as VEGF-R2 expression, improving the effects obtained by either drug used as monotherapy. Concordantly, it has been already shown that the functional block of VEGF-R2 and, hence, of VEGF itself in neuroblastoma xenograft models led to therapeutic effectiveness (53). Moreover, Stephan et al. showed that the combination of rapamycin and anti-VEGF antibodies inhibited primary and metastatic tumor growth in an orthotopic model of human pancreatic cancer (46).

The therapeutic relevance of the antiangiogenic aspect has been further underlined through the effectiveness of vinblastine and rapamycin in inhibiting angiogenesis induced *in vivo* by human neuroblastoma biopsy specimens grafted to chick embryo chorioallantoic membrane. The angiostatic activity was greatly increased by the combined therapy, with respect to monotherapy, in agreement with our previous data (16).

In conclusion, the association of vinblastine and rapamycin results in an increased antitumor effectiveness against neuroblastoma compared with either drug administered separately. The observed antitumor efficacy can be ascribed to inhibition of tumor cell proliferation and angiogenesis as well as apoptosis induction. These preclinical results can be relevant to design new therapeutic approaches against neuroblastoma.

Acknowledgments

We thank V. Pistoia for suggestions and revisions, F. Parodi for expert technical assistance, and C. Bernardini for editing.

References

1. Maris JM, Matthay KK. Molecular biology of neuroblastoma. J Clin Oncol 1999;17:2264–79.

2. De Bernardi B, Nicolas B, Boni L, et al. Disseminated neuroblastoma in children older than one year at diagnosis: comparable results with three consecutive high-dose protocols adopted by the Italian Co-Operative Group for Neuroblastoma. J Clin Oncol 2003;21:1592–601.

3. Rowinsky EK, Donehower RC. Microtubule-targeting drugs. In: Perry MC, editor. The chemotherapy source book. 2nd ed. Baltimore: Williams and Wilkins; 1998. p. 387–423.

4. Page AM, Hieter P. The anaphase-promoting complex: new subunits and regulators. Annu Rev Biochem 1999;68:583–609.

5. Schwartsmann G, Bender RA. *Vinca* alkaloids. Cancer Chemother Biol Response Modif 1988;10: 50–6.

6. Bostrom B, Woods WG, Ramsay NK, Krivit W, Levine P, Nesbit ME, Jr. Cisplatin, vinblastine, and bleomycin (CVB) therapy for relapsed disseminated neuroblastoma. Cancer Treat Rep 1984;68:1157–8.

7. Martel RR, Klicius J, Galet S. Inhibition of the immune response by rapamycin, a new antifungal antibiotic. Can J Physiol Pharmacol 1977;55:48–51.

8. Sehgal SN, Molnar-Kimber K, Ocain TD, Weichman BM. Rapamycin: a novel immunosuppressive macrolide. Med Res Rev 1994;14:1–22.

9. Douros J, Suffness M. New antitumor substances of natural origin. Cancer Treat Rev 1981;8:63–87.

10. Dumont FJ, Su Q. Mechanism of action of the immunosuppressant rapamycin. Life Sci 1996;58: 373–95.

11. Sehgal SN. Rapamune (RAPA, rapamycin, sirolimus): mechanism of action immunosuppressive effect results from blockade of signal transduction and inhibition of cell cycle progression. Clin Biochem 1998;31: 335–40.

12. Noh WC, Mondesire WH, Peng J, et al. Determinants of rapamycin sensitivity in breast cancer cells. Clin Cancer Res 2004;10:1013–23.

13. Kerbel RS, Viloria-Petit A, Klement G, Rak J. 'Accidental' anti-angiogenic drugs. anti-oncogene directed signal transduction inhibitors and conventional chemotherapeutic agents as examples. Eur J Cancer 2000;36:1248–57.

14. Vacca A, Iurlaro M, Ribatti D, et al. Antiangiogenesis is produced by nontoxic doses of vinblastine. Blood 1999;94:4143–55.

15. Guba M, von Breitenbuch P, Steinbauer M, et al. Rapamycin inhibits primary and metastatic tumor growth by antiangiogenesis: involvement of vascular endothelial growth factor. Nat Med 2002;8:128–35.

16. Marimpietri D, Nico B, Vacca A, et al. Synergistic inhibition of human neuroblastoma-related angiogenesis by vinblastine and rapamycin. Oncogene 2005; 24:6785–95.

17. Campostrini N, Marimpietri D, Totolo A, et al. Proteomic analysis of anti-angiogenic effects by a combined treatment with vinblastine and rapamycin in an endothelial cell line. Proteomics 2006;6:4420–31.

18. Doll DC, Ringenberg QS, Yarbro JW. Vascular toxicity associated with antineoplastic agents. J Clin Oncol 1986;4:1405–17.

19. Misawa A, Hosoi H, Tsuchiya K, Sugimoto T. Rapamycin inhibits proliferation of human neuroblastoma cells without suppression of MycN. Int J Cancer 2003;104:233–7.

20. Longo LD. [Transplacental gas exchange]. Rev Mal Respir 1988;5:197–206.

21. Cornaglia-Ferraris P, Ponzoni M, Montaldo P, et al. A new human highly tumorigenic neuroblastoma cell line with undetectable expression of N-*myc*. Pediatr Res 1990;27:1–6.

22. Bogenmann E. A metastatic neuroblastoma model in SCID mice. Int J Cancer 1996;67:379–85.

23. Biedler JL, Helson L, Spengler BA. Morphology and growth, tumorigenicity, and cytogenetics of human neuroblastoma cells in continuous culture. Cancer Res 1973;33:2643–52.

24. Gross N, Favre S, Beck D, Meyer M. Differentiation-related expression of adhesion molecules and receptors on human neuroblastoma tissues, cell lines and variants. Int J Cancer 1992;52:85–91.

25. Ponzoni M, Bocca P, Chiesa V, et al. Differential effects of *N*-(4-hydroxyphenyl)retinamide and retinoic acid on neuroblastoma cells: apoptosis versus differentiation. Cancer Res 1995;55:853–61.

26. Brignole C, Marimpietri D, Pastorino F, et al. Effect of bortezomib on human neuroblastoma cell growth, apoptosis, and angiogenesis. J Natl Cancer Inst 2006;98:1142–57.

27. Ribatti D, Alessandri G, Baronio M, et al. Inhibition of neuroblastoma-induced angiogenesis by fenretinide. Int J Cancer 2001;94:314–21.

28. Khanna C, Jaboin JJ, Drakos E, Tsokos M, Thiele CJ. Biologically relevant orthotopic neuroblastoma xenograft models: primary adrenal tumor growth and spontaneous distant metastasis. In Vivo 2002;16:77–85.

29. Pastorino F, Brignole C, Marimpietri D, et al. Vascular damage and anti-angiogenic effects of tumor vessel-targeted liposomal chemotherapy. Cancer Res 2003; 63:7400–9.

30. Pastorino F, Brignole C, Di Paolo D, et al. Targeting liposomal chemotherapy via both tumor cell-specific and tumor vasculature-specific ligands potentiates therapeutic efficacy. Cancer Res 2006;66:10073–82.

31. Brodeur GM, Pritchard J, Berthold F, et al. Revisions of the international criteria for neuroblastoma diagnosis, staging, and response to treatment. J Clin Oncol 1993;11:1466–77.

32. Ribatti D, Gualandris A, Bastaki M, et al. New model for the study of angiogenesis and antiangiogenesis in the chick embryo chorioallantoic membrane: the gelatin sponge/chorioallantoic membrane assay. J Vasc Res 1997;34:455–63.

33. Elias H, Hyde DM. Stereological measurements of isotropic structures. In: Elias H, Hyde DM, editors. In a guide to practical stereology. Basel: Karger; 1983. p. 25–44.

34. Meitar D, Crawford SE, Rademaker AW, Cohn SL. Tumor angiogenesis correlates with metastatic disease, N-*myc* amplification, and poor outcome in human neuroblastoma. J Clin Oncol 1996;14:405–14.

35. Ribatti D, Alessandri G, Vacca A, Iurlaro M, Ponzoni M. Human neuroblastoma cells produce extracellular matrix-degrading enzymes, induce endothelial cell proliferation and are angiogenic *in vivo*. Int J Cancer 1998;77:449–54.

36. VanderWeele DJ, Zhou R, Rudin CM. Akt up-regulation increases resistance to microtubule-directed chemotherapeutic agents through mammalian target of rapamycin. Mol Cancer Ther 2004;3:1605–13.

37. Wendel HG, De Stanchina E, Fridman JS, et al. Survival signalling by Akt and eIF4E in oncogenesis and cancer therapy. Nature 2004;428:332–7.

38. Fan M, Du L, Stone AA, Gilbert KM, Chambers TC. Modulation of mitogen-activated protein kinases and phosphorylation of Bcl-2 by vinblastine represent persistent forms of normal fluctuations at G2-1. Cancer Res 2000;60:6403–7.

39. Hidalgo M, Rowinsky EK. The rapamycin-sensitive signal transduction pathway as a target for cancer therapy. Oncogene 2000;19:6680–6.

40. Mondesire WH, Jian W, Zhang H, et al. Targeting mammalian target of rapamycin synergistically enhances chemotherapy-induced cytotoxicity in breast cancer cells. Clin Cancer Res 2004;10: 7031–42.

41. Geoerger B, Kerr K, Tang CB, et al. Antitumor activity of the rapamycin analog CCI-779 in human primitive neuroectodermal tumor/medulloblastoma models as single agent and in combination chemotherapy. Cancer Res 2001;61:1527–32.

42. Jordan MA, Wilson L. Microtubules and actin filaments: dynamic targets for cancer chemotherapy. Curr Opin Cell Biol 1998;10:123–30.

43. Brown JM, Attardi LD. The role of apoptosis in cancer development and treatment response. Nat Rev Cancer 2005;5:231–7.

44. Kroemer G, Martin SJ. Caspase-independent cell death. Nat Med 2005;11:725–30.

45. Ribatti D, Raffaghello L, Pastorino F, et al. *In vivo* angiogenic activity of neuroblastoma correlates with MYCN oncogene overexpression. Int J Cancer 2002; 102:351–4.

46. Stephan S, Datta K, Wang E, et al. Effect of rapamycin alone and in combination with antiangiogenesis therapy in an orthotopic model of human pancreatic cancer. Clin Cancer Res 2004;10:6993–7000.

47. Jin F, Xie Z, Kuo CJ, Chung LW, Hsieh CL. Cotargeting tumor and tumor endothelium effectively inhibits the growth of human prostate cancer in adenovirus-mediated antiangiogenesis and oncolysis combination therapy. Cancer Gene Ther 2005;12: 257–67.

48. Yoshiji H, Gomez DE, Shibuya M, Thorgeirsson UP. Expression of vascular endothelial growth factor, its receptor, and other angiogenic factors in human breast cancer. Cancer Res 1996;56:2013–6.

49. Brown LF, Berse B, Jackman RW, et al. Expression of vascular permeability factor (vascular endothelial growth factor) and its receptors in adenocarcinomas of the gastrointestinal tract. Cancer Res 1993;53: 4727–35.

50. Meister B, Grunebach F, Bautz F, et al. Expression of vascular endothelial growth factor (VEGF) and its receptors in human neuroblastoma. Eur J Cancer 1999;35:445–9.

51. Langer I, Vertongen P, Perret J, Fontaine J, Atassi G, Robberecht P. Expression of vascular endothelial growth factor (VEGF) and VEGF receptors in human neuroblastomas. Med Pediatr Oncol 2000;34: 386–93.

52. Fakhari M, Pullirsch D, Paya K, Abraham D, Hofbauer R, Aharinejad S. Upregulation of vascular endothelial growth factor receptors is associated with advanced neuroblastoma. J Pediatr Surg 2002;37: 582–7.

53. Klement G, Baruchel S, Rak J, et al. Continuous low-dose therapy with vinblastine and VEGF receptor-2 antibody induces sustained tumor regression without overt toxicity. J Clin Invest 2000;105: R15–24.